Preparation of Electrochemical and Magnetic properties of Manganese Ferrite nanoparticles via sol-gel auto combustion Method

S. Vinothkumar[1], P. Hajasharif *[1&2] and P. Sivagurunathan[1]

[1]*Department of Physics, Annamalai University, Annamalainagar-608 002, Tamil Nadu, India

[2]Department of physics, Arignar anna govt arts college Villupuram-605 602, Tamil Nadu, India

Corresponding author: hajasharif2k5@gmail.com

Abstract

The spinel structure of manganese ferrite nanoparticles has been successfully prepared by the sol-gel auto combustion method. The prepared manganese ferrite samples were characterized by TG/DTA, XRD, FE-SEM, HR-TEM, FTIR, VSM and CV. Studies are used were utilized to study the effect of synthetic methodology on the properties of synthesized nanoparticles. Structural parameters of prepared samples were carried out using the X-ray diffraction technique. XRD results present the single-phase manganese ferrite nanoparticles annealed at 700°C with an average crystalline size of about 15 nm. Field emission scanning electron microscopy pictures have shown that particles are spherical with less agglomerated. Results from high-resolution transmission electron microscopy ensured that the distinguished nanoparticles were of a crystalline nature. Magnetic behavior is analyzed on the saturation and remanence magnetization coercivity of single-phase manganese ferrite nanoparticles. The value of saturation magnetization is 87.01emu/g. The electrochemical study showed that the manganese ferrite nanoparticles have the specific capacitance values are 290.4 F/g at a sweep rate of 10 mv/s.

Keywords: *Sol-gel and auto combustion, Nano Ferrite, Magnetic and Electrochemical properties.*

1.Introduction

Spinel ferrites with the general formula AFe_2O_4 (A = Fe, Co, Ni, Cu, Mn) are very important magnetic materials because of their interesting magnetic and electrical properties with chemical and thermal stabilities [1]. There are interesting electrical and magnetic properties in the applications of spinel manganese ferrite. Manganese ferrite ($MnFe_2O_4$) is one among the compounds originally thought to be an inverse spinel, but later found to be 80% normal and 20% inverse structure. It has received considerable attention in microwave electronic storage and magnetic storage applications. It has a high magnetic permeability and electrical resistance. In order to obtain ferrite powders, a number of synthetic methods were developed. The other methods have several disadvantages, such as large and non-uniform particle size and impurities, which prevent further improvement in the performance of the products [2, 3]. Manganese ferrite ($MnFe_2O_4$) is also important to the ferrite family and is widely used in microwave and magnetic recording applications [4].

$MnFe_2O_4$ synthesized by this method can form homogeneous precursor and makes it have better performance as low coercivity, moderate saturation magnetization, good chemical stability, high permeability and mechanical hardness [5,6]. The preparation of spinel ferrite nanocrystals through different routes has become an essential focus of related research and development activities. Various fabrication methods to prepare spinel ferrites nanocrystals have been reported, such as, sol-gel methods [7], the ball-milling technique [8], co-precipitation [9], micro- emulsion process [10], the hydrothermal method [11], the reverse micelles process [12,13], and sol-gel auto combustion method, [14]. The synthesis of manganese ferrite is more difficult since the high sintering temperature is necessary. Among spinel ferrites, manganese ferrite ($MnFe_2O_4$) is a significant member of ferrite family having the spinel structure (AB_2O_4) with two divalent cation sites: 8 tetrahedral A sites and 16 octahedral B sites. Manganese ferrite has notable properties such as coercivity, moderate saturation magnetisation, super paramagnetism, good chemical stability, and mechanical hardness [15-17]. A typical ferrite of the spine is written MFe_2O_4 where M is a metal or a group of metal elements with two different values. The cations M^{2+} and Fe^{3+} shall be divided into tetrahedral crystals and octahedrons of the spine structure [18]. In the present investigation, ($MnFe_2O_4$) nanoparticles are synthesized by sol-gel auto combustion method. The structure, composition, thermal and magnetic properties of the gel precursor is characterized by XRD (X-ray diffraction), FE-SEM (Field Emission Scanning Electron Microscopy). HR-TEM (high-resolution transmission electron microscopy) the magnetic properties of the samples were studied using VSM (Vibrating Sample Magnetometer) and CV (Cyclic Voltammetry). In addition, the manganese ferrite sample synthesized from the analysis feature studies (TG-DTA, XRD, FE-SEM, HR-TEM, FTIR, VSM and CV).

2. Synthesis Procedure

2.1. Materials

For the preparation of manganese ferrite nanoparticles, metal nitrate reagents were used as precursors, citric acid was used as the chelating agent, and distilled water was used as the solvent. Ferric nitrate, ($Fe(NO_3)_3.9H_2O$) and manganese (II) nitrate, ($Mn(NO_3)_2$, are ethylene glycol ($HOCH_2CH_2OH$) were purchased from Merck chemicals by pure AR grade (99%) is used for the present work without any further purification.

2.2 Synthesis Procedure of Manganese Ferrite Nanoparticles

The synthesis of manganese ferrite nanoparticles by sol–gel auto combustion method shown in **Figure:1**, and the materials were purchased from merck chemical the synthesis nano material 0.1M mol manganese (II) nitrate (Mn((NO_3), 1.0M, Iron(III) nitrate nano hydrate ($Fe(NO_3)_3.9H_2O\_6H_2O$) from merck chemical company, and were dissolved in 20 ml ethylene glycol ($HOCH_2CH_2OH$) merck chemical was added under stirring to form a uniform solution. The mixed solution was sealed and heated to 120 C during 5 h - 6 h to obtain the gel products. The obtained gel solution obtained dried at 80 C for 3 hours to produce the nanomaterial the sample mole ratio X = 0.2M values were enumerated as manganese ferrite respectively.

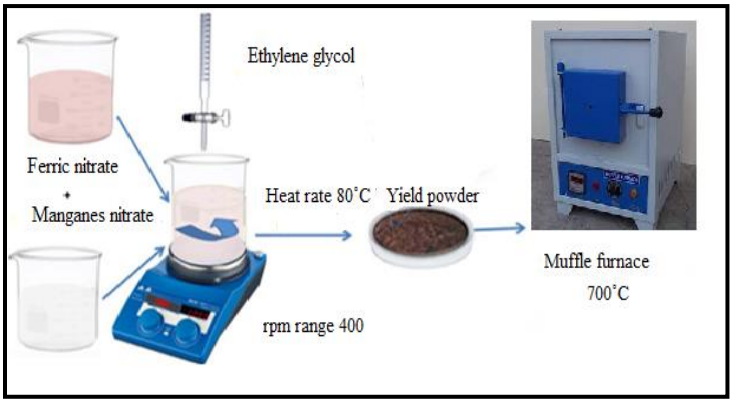

Fig.1. Synthesis Procedure of Manganese Ferrite

2.3 Characterization Techniques

The thermal stability of the powder sample determined by TG/DTA analysis was performed using NETZSCH-STA 449 F3 JUPITER from the Department of Physics CISL, Annamalai University, Chidambaram. Tamil Nadu. The manganese nanoparticles were found in crystalline phase purity of X-ray diffraction (XRD) technique using by PW3040 " X" pert PRO sample powder to the X-ray diffract meter with CuK α radiation (λ = 1.54060Å) at 40 kV and 30 mA. Step scans recorded for values of 2θ in the 20 to 80 angular range with a sweep speed of 10 min^{-1}. The surface morphology of the nanoparticles was exposed through field emission scanning electron microscopy used by ZEISS SUPRA-55 VP: FE-SEM from Sathyabama University, Chennai. The Morphology and shape with determining the size of the sample powder particles using VIT Vellore's (High Resolution Transmission Electron Microscope. The selected areas of the electron diffraction patterns (SEAD) were recorded by dispersing the sample onto a carbon-covered copper grid. The powder sample analysis was Functional groups and the composition of the synthesized sample revealed through FT-IR measurements using thermo nicolet iS5 FTIR- spectroscopy instruments department of chemistry , Annamalai university Annamalai nagar Tamilnadu. The sample was analyzed for magnetization using the LAKESHORE VSM 7410 instruments of the SAIF labourites, kowhatti of the respective. The electrochemical properties were performed on a model CHI 660 by cyclic Voltammetry (CV) using three electrode systems in 2 M KOH electrolyte solutions at room temperature.

3. Results and Discussion

3.1 Thermal study (TG/DTA)

Synchronized thermo gravimetric and differential thermal analyses (TG/DTA) of the As- prepared samples is performed in the temperature range from 38 ºC to 1000 ºC at the rate of 20 ºC/ minute. TG/DTA study of the as-prepared product is shown in **Fig:2**. It has been measured three predictable weight losses from the TG curve. The first weight losses are observed in the range 100 ºC to 250 ºC (3 %) is due to desorption of water molecules. The second weight losses of (21 %) have been observed in the range of 250 ºC to 320 ºC owing to the decomposition of nitrate and other organic templates. The third weight losses of (8 %)

observed in the range 320 ºC to 380 ºC due to the phase transitions of the sample. No weight losses are predicted beyond 685 ºC confirms the formation of manganese ferrite nanoparticles [19, 20]. The DTA curve shows a small endothermic peak at 250 ºC is due to the desorption of water molecules. The endothermic peak observed in the range 380 ºC is due to the decomposition of nitrates in the synthesized sample [21].

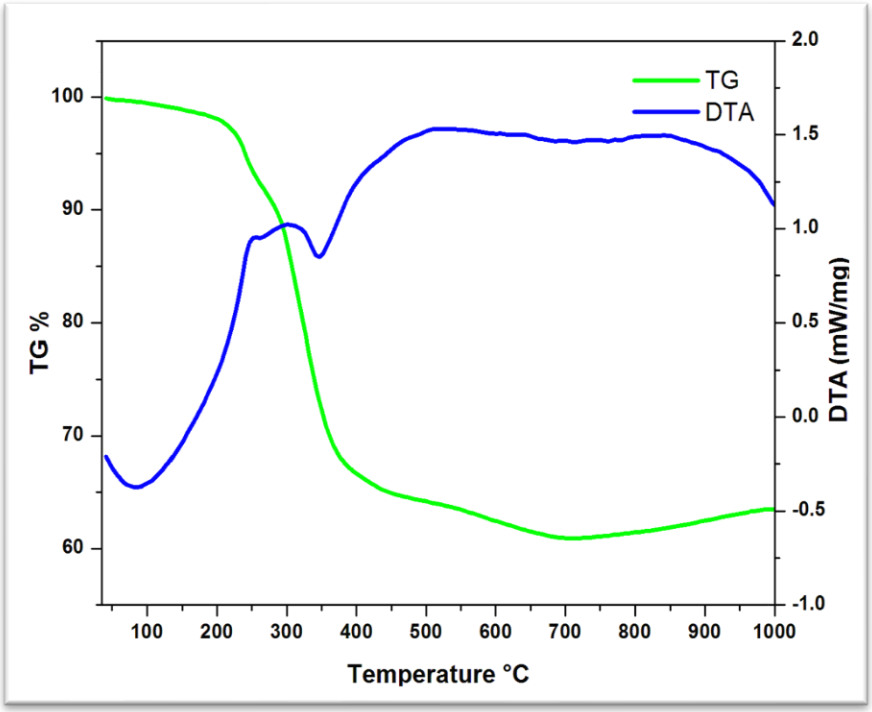

Fig2.TG/DTA of the manganese ferrite nanoparticles

3.2 X-Ray Diffraction Study (XRD)

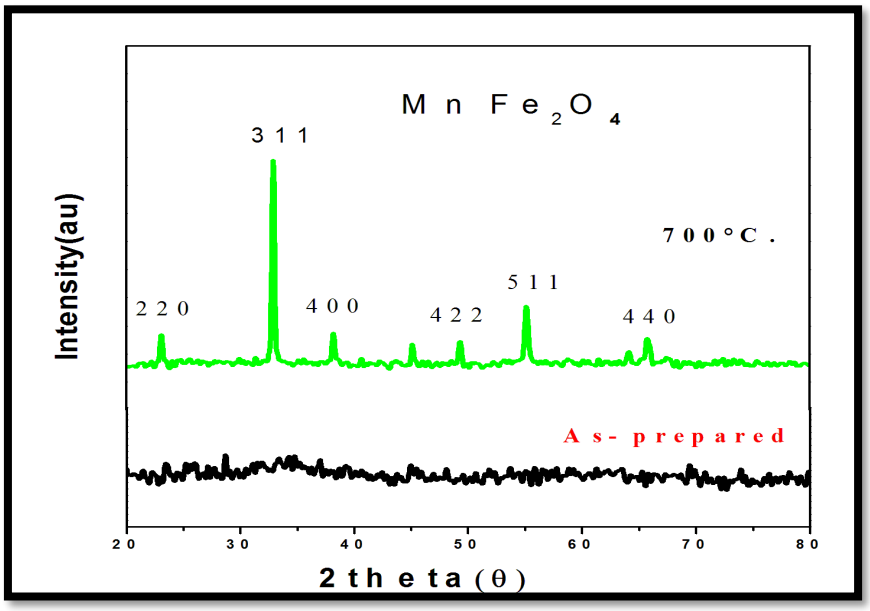

Fig:3. XRD analysis of the $MnFe_2O_4$ nanoparticles

X- ray diffraction analysis of the as–prepared and annealed at manganese ferrite nanoparticles at 700 ºC is shown in **Fig.3**. In this fig.3 as- prepared powder does not show any crystalline peaks and confirms that annealing is essential to stability the crystalinity and preventing their agglomeration. The XRD graph of the annealed samples, exhibits the reflections with h,k,l values of (220), (311), (400), (422), (511), and (440) planes specify the cubic phase with space group Fd3m . The major plane (311) is due to the prominence of the manganese ferrite phase. The achieved XRD peaks are well matched with the standard characteristic peaks of the manganese ferrite samples are reported in JCPDS, File No #(73-2410). The observed peaks in the current work obviously designate the formation of manganese ferrite nanoparticles without any other impurities. The reflected pattern are sharp and intense peaks showed in the XRD pattern indicated a high degree of crystalline of synthesized X- ray diffraction of manganese ferrite nanoparticles. The mean crystallite size was determined from the full width at half maximum (FWHM) using the well-known Debye–Scherer's formula $D= 0.9\lambda/\beta\cos\theta$ where D is the crystalline size (nm), β is the full width at half the maximum intensity measured in radians, λ is the X-ray wavelength of Cu Kα =0.1546 nm, and θ is the Bragg angle. The mean crystallite size has been calculated using Debye–Scherer's formula and the observed values are 15 nm for 700°C respectively [22-24]. In the mixed spinel structure of manganese ferrite nanoparticles showed the existence of Mn^{2+} and Fe^{3+} ions in the sub-lattices of A and B. Lattice parameter "a" can be calculated by using the relation

$$a = d_{hkl} (h^2+k^2+l^2)^{1/2}.$$

The "a" value is observed are 8.9780 A° for manganese ferrite nanoparticles [25]. The value of crystallite size and lattice parameter are tabulated in **Table 1.**

Table 1. Structural parameter of $MnFe_2O_4$ nanoparticles annealed at 700°C

Sample temperature	D(nm)	Lattice parameter (a)
700°C	15 nm	8.9780 A°

3.3FE-SEM with EDAX Study

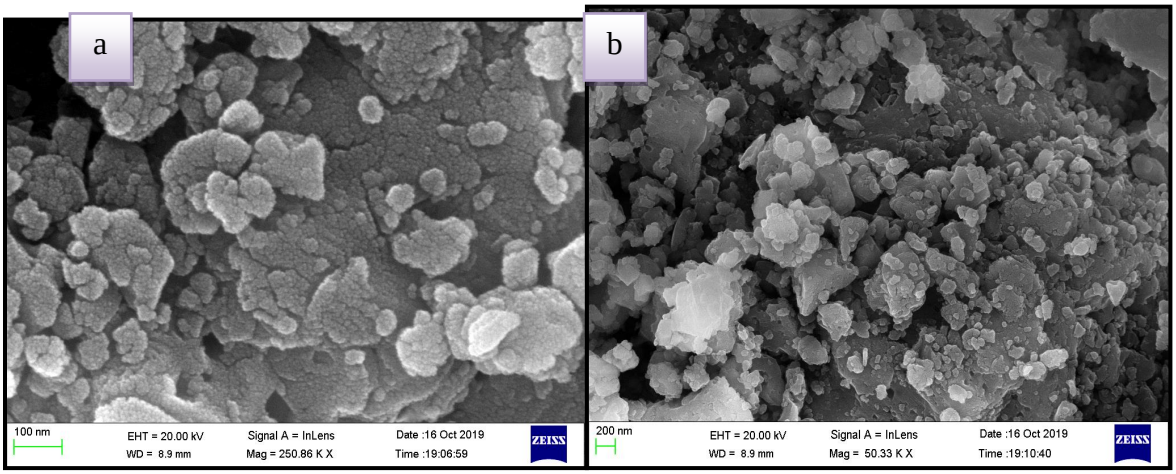

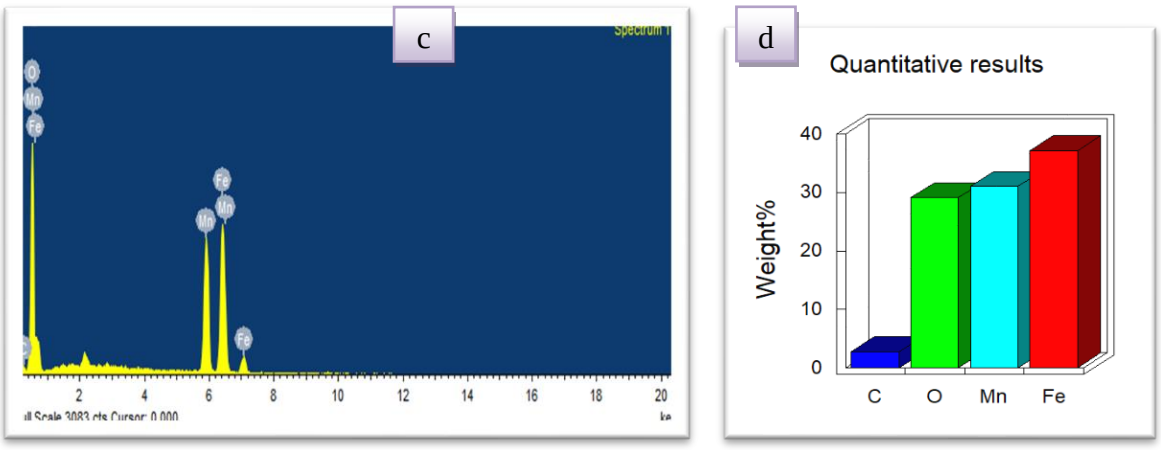

Fig.4(a),(b), FE-SEM images and (c),(d) EDAX and Quantitative analysis of the manganese ferrite nanoparticles

The morphology of the manganese ferrite nanoparticles annealed at 700°C was investigated through FE-SEM images and EDAX and Quantitative analysis of the manganese ferrite nanoparticles as shown in **Fig:4** (a, b, c, d). A surface morphology of manganese ferrite nanoparticles was analyzed by FE-SEM as shown in **Fig:4.(a, b)** of the morphology image shows that particles are shape of spherical. It is dependent on the intermolecular force between nanoparticles and cumulative behavior of nanoparticles [26]. The appearance of some agglomerated species in the FE-SEM image was due to the naturally happening interaction between magnetic nanoparticles. The elemental composition of the synthesized manganese ferrite nanoparticles is determined using EDAX spectrum. From the EDAX result, the spectra contain the presence of Mn, Fe and O and the corresponding histogram of weight percentage are shown in **figure 4c** shows an EDAX pattern of manganese ferrite nanoparticles. The manganese ferrite of the atomic weight of Mn, Fe and O was obtained as 31.04 (At%), 37.13 (At%) and 29.09 (At%) indicating a good stoichiometric ratio of ~1:2 (Mn: Fe) in spinal structured manganese ferrite[27].

3.4HR-TEM Study

HR-TEM was used to analyze the particle size and shape. TEM images of the catalysts produced for this study are shown in Figure 4. While the catalysts were variable in shape and size, the majority were spherical in nature with size ranging from 20 to 100 nm. In the presence of studies the agglomeration of prepared manganese ferrite samples is magnetic interaction between the nanoparticles.

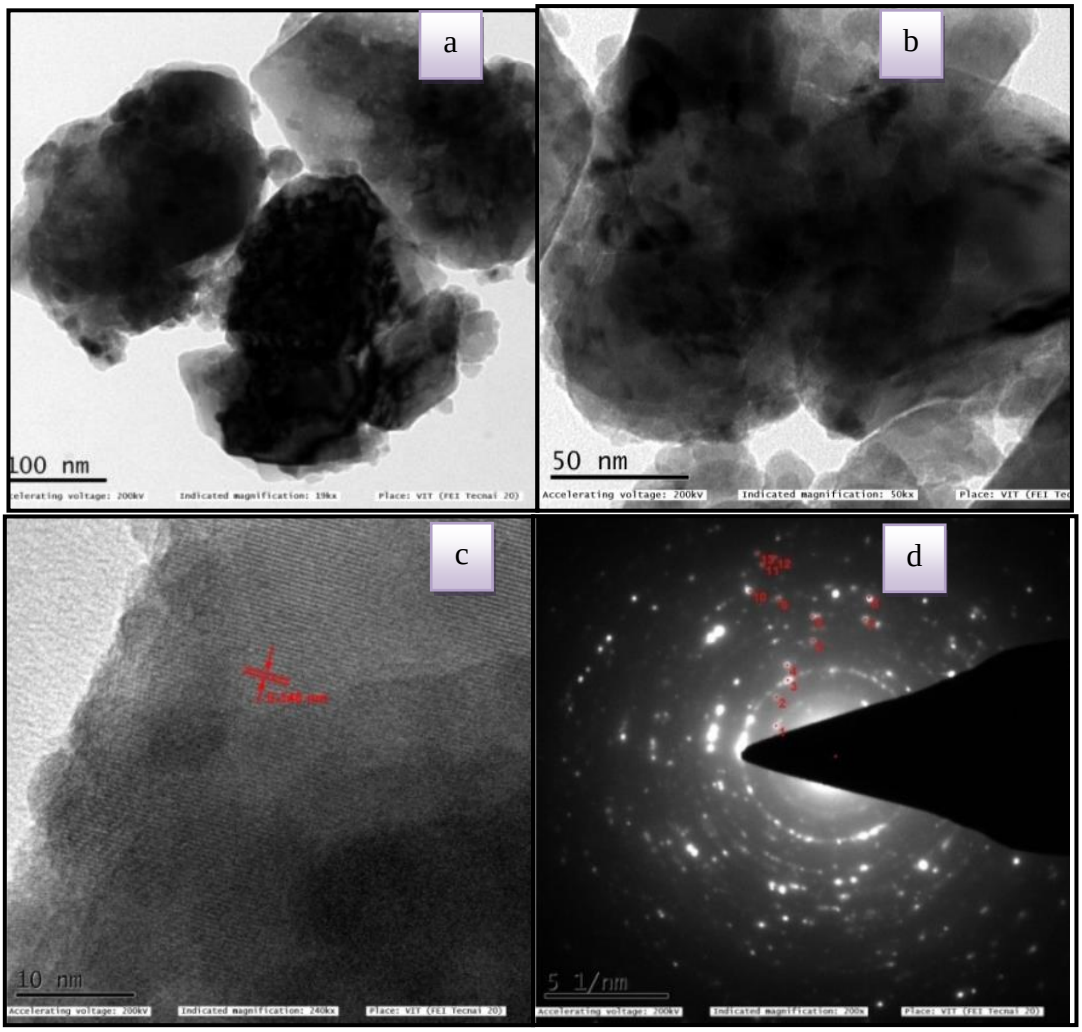

Fig:5 (a), (b), (c) HRTEM images and corresponding (d) SAED pattern of the manganese ferrite nanoparticles

The average particle size was found to be 15 nm, the length of the individual selected particles measured in images j viewer software is shown in **Figure:5, (a, b, c)** and HR-TEM images analysis estimated particle size, which is in good agreement with the XRD result [28]. **Fig.5 (d)** shows the selected area electron diffraction (SAED) pattern repressing sharp rings, which reveal the good crystalline of the manganese ferrite nanoparticles.

3.5 FTIR Study

Fig:6, Indicate that the FTIR spectrum of manganese ferrite nanoparticles annealed at 700°C were recorded in the range of 4000-400 cm^{-1} by kBr pellet technique through the solid phase the increased annealing temperature and the disappearance of the absorption band at 1320 to 1460 cm^{-1} could be attributed to the complete decomposition of the nitrates and also, the intensity of O-H vibration of water molecules are 1460.89 and 3423-3698.37 cm^{-1}. In this work, the two absorption band between the regions 400-600 cm^{-1}, this corresponds to the octahedral site of $MnFe_2O_4$ nanoparticles. In which the higher absorption band around υ_1= 571.99 cm^{-1} corresponds to the stretching vibrations of tetrahedral complexes of Mn-O/ Fe- O and the lower absorption band around υ_2=415 cm^{-1} is attributed to the vibration of octahedral groups Fe-O is shown and listed in Table:2 [29].

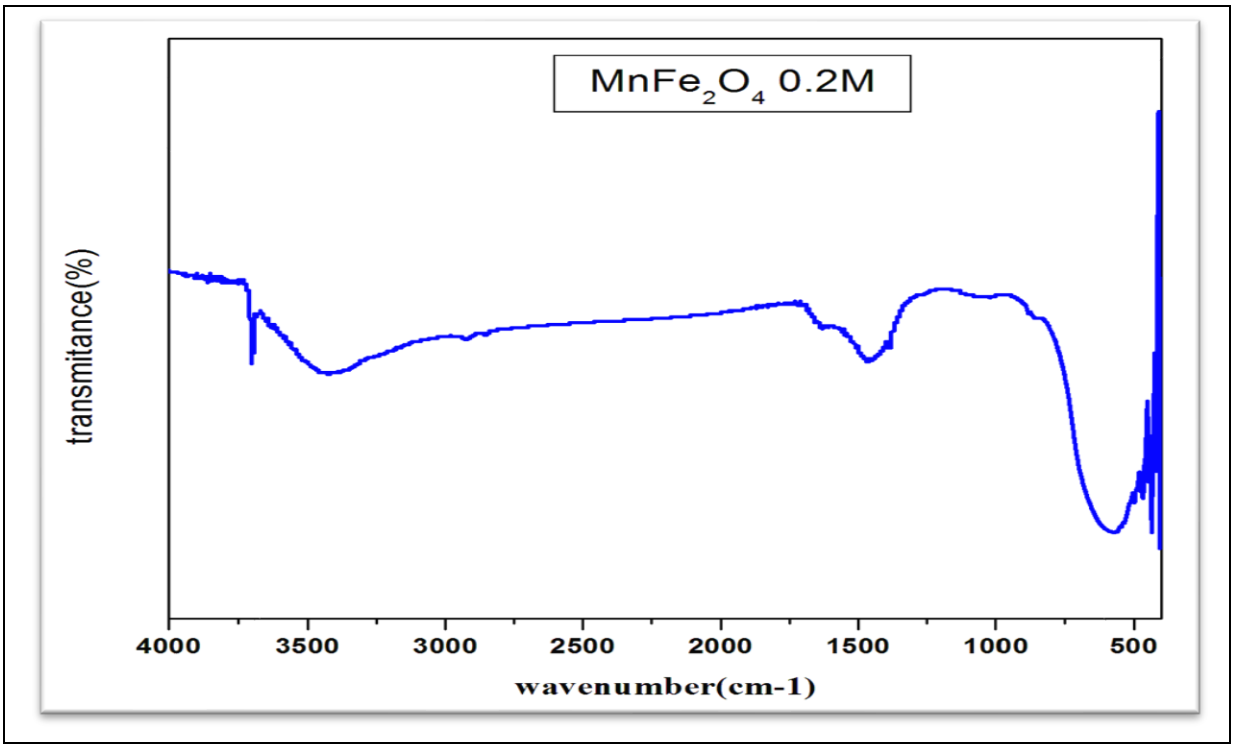

Fig.6 FTIR spectrum of manganese ferrite nanoparticles of 700°C temperatures

Table2. The absorption band of manganese ferrite nanoparticles annealed at 700°C

Annealed temperature (°C.)	υ_1	υ_2
700	571.99 cm^{-1}	415 cm^{-1}

3.6 VSM Study

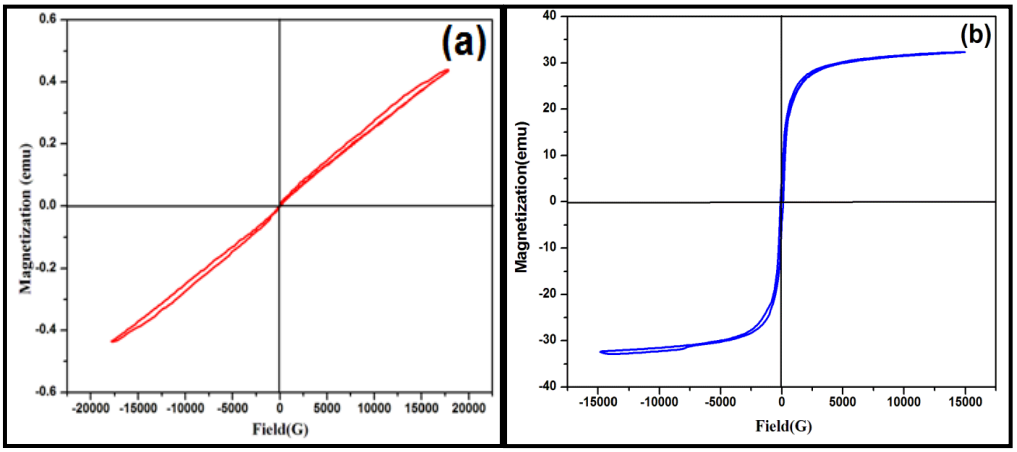

Fig:7. (a) as-prepared and (b) annealed at 700 °C of the manganese ferrite nanoparticles

Fig.6 shows the magnetic hysteresis was performed at RT in the magnetization range of 20 to +20 kOe. Various magnetic parameters such as, magnetization (Ms), remanence (Mr) and coercivity (Hc) were presented in **Table:3**. From the table illustrates that the saturation magnetization of as prepared and annealed samples increasing magnetic increases. As it clear from the as-prepared manganese ferrite nanoparticle are shown in **Fig:7 (a)** demonstrate the

super paramagnetic nature of samples. The annealed manganese ferrite sample shows ferromagnetic structure in **Fig:7 (b)**. Saturation magnetization was calculated given by

$$(Ms) = Ms / M$$

Where "Ms" is a magnetization of the sample, "M" is a total mass of the sample. The as-prepared and annealing temperature of saturation magnetization increased from 1.27 to 87.01 emu/g. The saturation magnetization of present samples is smaller than that (80 emu/g) of bulk manganese ferrite materials [30]. This can be attributed to spin canting and surface spin disorder that occurred in these nanoparticles [31]. The interactions between A and B sub-lattices in the spinel lattice system (AB_2O_4) consist of inter-sub-lattice (A–B) super exchange interactions and intra-sub-lattice (A–A) and (B–B) exchange interactions. Inter-sub-lattice super-exchange interactions of the cations on the (A–B) are much stronger than the (A–A) and (B–B) intra-sub-lattice exchange interactions [32, 33]. Li et al., 2010 have reported with increasing the calcinations temperature of the manganese ferrite nanoparticles, Fe^{3+} ions transferred from B site to A site, so the accumulation of Fe^{3+} ions increased in A site; however, the Fe^{3+} at A site and Fe^{3+} at B site super-exchange interactions increased interactions were twice as strong as the Mn^{2+} at A site and Fe^{3+} at B site interactions, and this can lead to an increase in saturation magnetization in manganese ferrite nanoparticles [34]. The hysteresis loops show high coactivity 122.21 Oe (Hc), saturation magnetization 87.01emu/g (Ms) and remanence 5.3emu/g) (Mr). From the curve, we analyses that fine particles are easier to be thermally activated to overcome the magnetic anisotropy.

Table 3 (a) As-prepared and (b) annealed 700 °C samples of the manganese ferrite nanoparticles

Samples	Ms (emu/g)	Mr (emu/g)	Hc (Oe)
As – prepared	1.2783	730.08	13.859 Oe
700°C	87.01	5.3	122.21 Oe

3.7 Cyclic Voltammetry Study

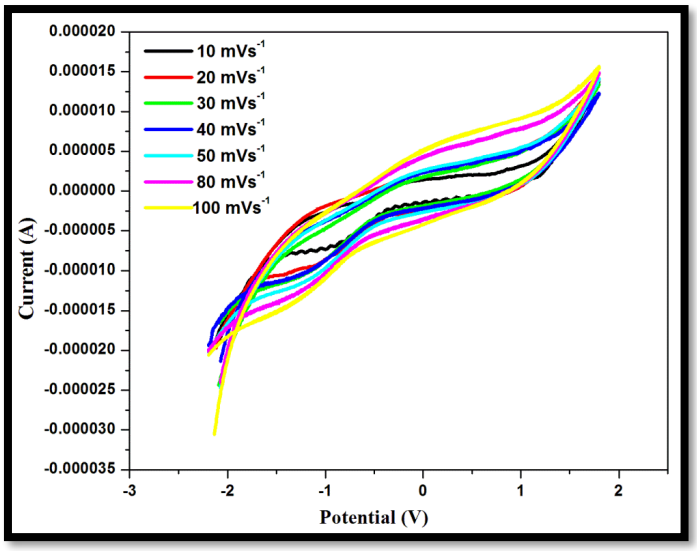

Fig.8 cyclic voltammetry study of manganese ferrite nanoparticles

Figure 7, reveals that the cyclic voltammetry study $MnFe_2O_4$ electrode were carried out at various scan rates of 10, 20, 30,40,30,40,50,80, and 100 mV/s. The shape of the cyclic voltammetry curves is an ideal rectangular shape observed at 10 mV/s. Further increasing the scan rate the observed pattern of the CV curve is altered and it confirms the pseudo capacitive nature of the material**.** The specific capacitance (SC) values of manganese ferrite electrode can be estimated by using the formula [35]

$$\mathbf{Cs = Q / m\Delta V}$$

Where, Cs is the specific capacitance, Q the anodic and cathodic charges on each scanning, m is the mass of the electrode material (mg) and ΔV is the scan rate (mVs^{-1}). Electrochemical measurements were performed in 0.2 tetra butyl ammonium perchlorate with a standard three electrode configuration consisting of a sample (working electrode), an Ag/ AgCl (reference electrode) and a high platinum wire (counter electrode) [36,37]. The scan rate increased in the range from 10 mV/s to 100mV/s and its corresponding specific capacitance values depicted in **Fig:8 and table:4** Further, the specific capacitance values of 290.4 F/g observed in the scan rate of 10 mV/s for the sample annealed at 700°C. The reason for high specific capacitance at low scan rate is observed in the present study suggested that the ionic diffusion takes place both inner and outer surfaces. The higher specific capacitance values observed in the present study confirm the good crystalinity of the manganese ferrite nanoparticles.

Table4. Specific capacitance values of manganese ferrite nanoparticles annealed at 700°C

Various scans rate mV/s	10	20	30	40	50	80	100
Specific capacitance F/g	290.4	196.3	143.1	124.5	106.9	46.8	19.19

4. Conclusion

The manganese ferrite nanoparticles were successfully synthesized by sol-gel auto combustion method. An XRD study reveals the phase identification of cubic structure with Fd3m space group. The FESEM result of manganese ferrite nanoparticles annealed at 700°Cshowed the presence of individual particles with a small agglomeration at some point. The HR-TEM image shows that the particles have a spherical morphology with a size distribution of 15 nm. The specific capacitance values of 290.4 F/g were observed in the lower scan rate at 10 mV/s from the CV study, which is found suitable for super capacitance application .The magnetic study of annealed manganese ferrite nanoparticles is ferromagnetic order. These materials are good manganese ferrite magnetic storage application.

References:

1. Barkatt, A., 1996. Magnetic Ceramics By Raul Valenzuela (National University of Mexico). Cambridge University Press: Cambridge, UK 1994. xix+ 312 pp. $79.95. ISBN 0-521-36485-X.
2. Ahmed, Y.M.Z., 2010. Synthesis of manganese ferrite from non-standard raw materials using ceramic technique. *Ceramics International*, *36*(3), pp.969-977.
3. Kadu, A.V., Jagtap, S.V. and Chaudhari, G.N., 2009. Studies on the preparation and ethanol gas sensing properties of spinel Zn0. 6Mn0. 4Fe2O4 nanomaterials. *Current Applied Physics*, *9*(6), pp.1246-1251.

4. Vestal, C.R. and Zhang, Z.J., 2003. Effects of surface coordination chemistry on the magnetic properties of MnFe2O4 spinel ferrite nanoparticles. *Journal of the American Chemical Society*, *125*(32), pp.9828-9833.
5. Cruz, M.M., Ferreira, L.P., Ramos, J., Mendo, S.G., Alves, A.F., Godinho, M. and Carvalho, M.D., 2017. Enhanced magnetic hyperthermia of CoFe2O4 and MnFe2O4 nanoparticles. *Journal of Alloys and Compounds*, *703*, pp.370-380.
6. Shanmugavel, T., Raj, S.G., Kumar, G.R. and Rajarajan, G., 2014. Synthesis and structural analysis of nanocrystalline MnFe2O4. *Physics Procedia*, *54*, pp.159-163.
7. Thakur, A. and Singh, M., 2003. Preparation and characterization of nanosize Mn0. 4Zn0. 6 Fe2O4 ferrite by citrate precursor method. *Ceramics International*, *29*(5), pp.505-511..
8. Aslibeiki, B., Kameli, P., Salamati, H., Eshraghi, M. and Tahmasebi, T., 2010. Superspin glass state in MnFe2O4 nanoparticles. *Journal of Magnetism and Magnetic Materials*, *322*(19), pp.2929-2934..
9. Bujoreanu, V.M., Diamandescu, L. and Brezeanu, M., 2000. On the structure of manganese ferrite powder prepared by coprecipitation from MnO2 and FeSO4· 7H2O. *Materials letters*, *46*(2-3), pp.169-174.
10. Uskoković, V. and Drofenik, M., 2005. A mechanism for the formation of nanostructured NiZn ferrites via a microemulsion-assisted precipitation method. *Colloids and Surfaces A: Physicochemical and Engineering Aspects*, *266*(1-3), pp.168-174.
11. Liu, C., Zou, B., Rondinone, A.J. and Zhang, Z.J., 2000. Reverse micelle synthesis and characterization of superparamagnetic MnFe2O4 spinel ferrite nanocrystallites. *The Journal of Physical Chemistry B*, *104*(6), pp.1141-1145.
12. Komarneni, S., Fregeau, E., Breval, E. and Roy, R., 1988. Hydrothermal preparation of ultrafine ferrites and their sintering. *Journal of the American Ceramic Society*, *71*(1), pp.C-26.
13. Liu, C. and Zhang, Z.J., 2001. Size-dependent superparamagnetic properties of Mn spinel ferrite nanoparticles synthesized from reverse micelles. *Chemistry of Materials*, *13*(6), pp.2092-2096.
14. Gabal, M.A., Abdel-Daiem, A.M., Al Angari, Y.M. and Ismail, I.M., 2013. Influence of Al-substitution on structural, electrical and magnetic properties of Mn–Zn ferrites nanopowders prepared via the sol–gel auto-combustion method. *Polyhedron*, *57*, pp.105-111.
15. Yang, H., Zhang, C., Shi, X., Hu, H., Du, X., Fang, Y., Ma, Y., Wu, H. and Yang, S., 2010. Water-soluble superparamagnetic manganese ferrite nanoparticles for magnetic resonance imaging. *Biomaterials*, *31*(13), pp.3667-3673.
16. Rondinone, A.J., Liu, C. and Zhang, Z.J., 2001. Determination of magnetic anisotropy distribution and anisotropy constant of manganese spinel ferrite nanoparticles. *The Journal of Physical Chemistry B*, *105*(33), pp.7967-7971.
17. Carta, D., Casula, M.F., Falqui, A., Loche, D., Mountjoy, G., Sangregorio, C. and Corrias, A., 2009. A structural and magnetic investigation of the inversion degree in ferrite nanocrystals MFe2O4 (M= Mn, Co, Ni). *The Journal of Physical Chemistry C*, *113*(20), pp.8606-8615.

18. Galindo, R., Mazario, E., Gutiérrez, S., Morales, M.P. and Herrasti, P., 2012. Electrochemical synthesis of NiFe2O4 nanoparticles: Characterization and their catalytic applications. *Journal of alloys and compounds*, *536*, pp.S241-S244.
19. Sahoo, Y., Pizem, H., Fried, T., Golodnitsky, D., Burstein, L., Sukenik, C.N. and Markovich, G., 2001. Alkyl phosphonate/phosphate coating on magnetite nanoparticles: a comparison with fatty acids. *Langmuir*, *17*(25), pp.7907-7911.
20. Swami, A., Kumar, A. and Sastry, M., 2003. Formation of water-dispersible gold nanoparticles using a technique based on surface-bound interdigitated bilayers. *Langmuir*, *19*(4), pp.1168-1172.
21. Yee, C., Kataby, G., Ulman, A., Prozorov, T., White, H., King, A., Rafailovich, M., Sokolov, J. and Gedanken, A., 1999. Self-assembled monolayers of alkanesulfonic and-phosphonic acids on amorphous iron oxide nanoparticles. *Langmuir*, *15*(21), pp.7111-7115.
22. Kim, J.G., Seo, J.W., Cheon, J.W. and Kim, Y.J., 2009. Rietveld analysis of nano-crystalline MnFe 2 O 4 with electron powder diffraction. *Bulletin of the Korean Chemical Society*, *30*(1), pp.183-187.
23. Lee, H.O., Kim, E.M., Yu, H., Jung, J.S. and Chae, W.S., 2009. Advanced porous gold nanofibers for highly efficient and stable molecular sensing platforms. *Nanotechnology*, *20*(32), p.325604.
24. Sugimoto, M., 1999. The past, present, and future of ferrites. *Journal of the American Ceramic Society*, *82*(2), pp.269-280.
25. *Lide, D.R. and Milne, G.W., 1995. Handbook of data on common organic compounds. CRC press.*
26. Ma, M., Zhang, Y., Yu, W., Shen, H.Y., Zhang, H.Q. and Gu, N., 2003. Preparation and characterization of magnetite nanoparticles coated by amino silane. *Colloids and Surfaces A: physicochemical and engineering aspects*, *212*(2-3), pp.219-226.
27. Pankaj Singh Rawat1, a), R. C. Srivastava1, Gagan Dixit1, G. C. Joshi1, K. Asokan2
28. Zeng, H., Rice, P.M., Wang, S.X. and Sun, S., 2004. Shape-controlled synthesis and shape-induced texture of MnFe2O4 nanoparticles. *Journal of the American Chemical Society*, *126*(37), pp.11458-11459.
29. Rani, S. and Varma, G.D., 2015. Superparamagnetism and metamagnetic transition in Fe3O4 nanoparticles synthesized via co-precipitation method at different pH. *Physica B: Condensed Matter*, *472*, pp.66-77.
30. Bozorth, R.M., Tilden, E.F. and Williams, A.J., 1955. Anisotropy and magnetostriction of some ferrites. *Physical Review*, *99*(6), p.1788.
31. Gu, Z., Xiang, X., Fan, G. and Li, F., 2008. Facile synthesis and characterization of cobalt ferrite nanocrystals via a simple reduction− oxidation route. *The Journal of Physical Chemistry C*, *112*(47), pp.18459-18466.
32. Atif, M., Hasanain, S.K. and Nadeem, M., 2006. Magnetization of sol–gel prepared zinc ferrite nanoparticles: effects of inversion and particle size. *Solid State Communications*, *138*(8), pp.416-421.
33. Ammar, S., Jouini, N., Fiévet, F., Beji, Z., Smiri, L., Moliné, P., Danot, M. and Grenèche, J.M., 2006. Magnetic properties of zinc ferrite nanoparticles synthesized by

hydrolysis in a polyol medium. *Journal of Physics: Condensed Matter*, *18*(39), p.9055.

34. Li, J., Yuan, H., Li, G., Liu, Y. and Leng, J., 2010. Cation distribution dependence of magnetic properties of sol–gel prepared MnFe2O4 spinel ferrite nanoparticles. *Journal of Magnetism and Magnetic Materials*, *322*(21), pp.3396-3400.
35. Kumar, C.R., Santosh, M.S., Nagaswarupa, H.P., Prashantha, S.C., Yallappa, S. and Kumar, M.A., 2017. Synthesis and characterization of β-Ni (OH) 2 embedded with MgO and ZnO nanoparticles as nanohybrids for energy storage devices. *Materials Research Express*, *4*(6), p.065503.
36. M.R. Anil Kumar, Buzuayehu Abebe, H.P. Nagaswarupa, H.C. Ananda Murthy, C.R.Ravikumar & Fedlu Kedir Sabir, "Enhanced photocatalytic and electrochemical performance of TiO2-Fe2O3 nanocomposite: Its applications in dye decolorization andas supercapacitors," Scientific Reports, Nature 10 (2020) 1249.
37. Raveesha, H.R., Nayana, S., Vasudha, D.R., Begum, J.S., Pratibha, S., Ravikumara, C.R. and Dhananjaya, N., 2019. The electrochemical behavior, antifungal and cytotoxic activities of phytofabricated MgO nanoparticles using Withania somnifera leaf extract. *Journal of Science: Advanced Materials and Devices*, *4*(1), pp.57-65.